Lasers in the Life Sciences 1(4), 1987, pp. 309–334

Angular Dependence of HeNe Laser Light Scattering by Human Dermis

S. L. JACQUES,† C. A. ALTER,† and S. A. PRAHL‡

†Department of Dermatology, Massachusetts General Hospital, Harvard Medical School, Boston, MA
‡Biomedical Engineering Program, University of Texas, Austin, TX

A goniometric apparatus is presented for measuring the angular dependence of scattering of a HeNe laser beam by *in vitro* human dermis samples of various thicknesses, hydrated to an 85 percent water content. Measurements of the transmitted and reflected light as a function of angle are presented for tissue thicknesses of 20–650 μm. Extrapolation of these angular scattering patterns to the limit of an incremental tissue thickness specifies the scattering phase function appropriate for use in the radiative transport equation. The scattering phase function is composed of a forward-directed scattering component (90 percent contribution) characterized as a Henyey-Greenstein function with g_{HG} equal 0.91, and an additional isotropic component (10 percent contribution, $b = 0.10$). The net value for the average cosine of the scattering phase function, g equal $(1 - b)g_{HG}$, is 0.82, which corresponds to an average deflection angle of 35° for a scattering event. The on-axis attenuation of the collimated HeNe laser beam indicates a total attenuation constant of 190 cm^{-1}, composed of an absorption coefficient of 2.7 cm^{-1} and a scattering coefficient of 187 cm^{-1}.

INTRODUCTION

The high intensity of laser radiation requires understanding of the propagation of light in tissue for intelligent choice of dosimetry in medical laser applications. Explosive vaporization can occur when temperatures exceed 100°C. Collagen denaturation and subsequent scarring occur between 60–

This work was supported by NIH grant AM25395-08, Office of Naval Research Contract #N0014-86K-0017, and the Arthur O. and Gullan M. Wellman Foundation.

Address correspondence to: Steven L. Jacques, Ph.D., Wellman Laboratory, Department of Dermatology, Massachusetts General Hospital, Boston, MA 02114.

70°C. Denaturation and irreversible aggregation of enzymes and other function proteins occur above 40–50°C. The distribution of primary tissue damage and subsequent biological response depends on the propagation of the treatment laser beam.

Light scattering in turbid tissues (*e.g.* dermis) can increase the light intensities within a tissue above that anticipated by simple exponential decay of the incident light (Beer's law). For example, a study of photocoagulation of mouse dermis by argon laser radiation indicated that heat deposition at a depth of 45 μm should be twice that expected at the surface based on the incident flux and Beer's law [1]. Subsurface hot spots can occur when scattered light within the tissue augments incident collimated light. Such subsurface hot spots can cause explosive vaporization which is quite destructive, the so-called "popcorn" effect [2].

Laser applications in medicine often attempt to affect targets buried in tissue. For example, the use of a pulsed tunable dye laser to selectively damage subsurface swollen blood vessels during portwine stain therapy requires a knowledge of light dosage at various depths in dermis [3–5]. Understanding the transition from an intense collimated beam to a diffuse light flux in human skin is a problem of current interest as protocols for laser phototherapy are developed.

The Kubelka-Munk diffuse flux model has been applied to skin optics [6–7], but such diffuse light experiments are not directly pertinent to the propagation of collimated light from a laser. Modification of the Kubelka-Munk model to consider an incident collimated light flux which scatters into forward and backward diffuse fluxes improves on the original model [8]. However, such a model inadequately describes the gradual transition from collimated to diffuse light, since light is assumed to be either collimated or totally diffuse. As will be shown in this report, laser light does not scatter isotropically in dermis, but is scattered primarily in the forward direction and slowly becomes diffuse with increasing depth.

For visible radiation, the transition of light from collimated to diffuse occurs in the first few hundred μm of penetration in the tissue, which is exactly that region most critical in many medical applications. Consequently, knowledge of the scattering function that characterizes a tissue is important. The scattering function describes the intensity of light scattered from an object as a function of angle between the incident direction and the scattered direction. This is commonly referred to as the single particle phase function used in the transport equation, and, for example, is used by Ishimaru in the 1D diffusion approximation solution to the transport equation [9]. This report

presents direct goniometric measurements of the phase function for light scattering in human dermis.

The angular dependence of light scattered from a target can be experimentally measured with a goniometer. Such measurements have provided useful information about light scattering in the epidermis of human skin [10] and in pig muscle [11]. This paper reports experimental measurements of the angular dependence of light scattering by thin human dermis samples of various thicknesses. The experiments were conducted with a HeNe laser at 632.8 nm, since scattering at this wavelength is representative for scattering in the spectral range 600–1300 nm [7], which is the "therapeutic window" that allows deep penetration of light into tissues [12]. The results obtained are pertinent to photodynamic therapy with hematoporphyrin derivative (HpD) using 630 nm laser radiation.

METHODS

Tissue Preparation

All experiments involved *in vitro* human skin samples obtained from autopsy for the sole purpose of this study. Caucasion skin samples from 50 to 70 y.o. subjects were obtained from autopsy.

In the first set of experiments, skin samples were obtained by dermatome at autopsy from the front of the leg (shin). Skin from this location is not used for skin transplants during burn therapy, and therefore was available for study. Samples from several subjects were studied during the development of this instrumentation and yielded similar results. The results from the final one subject are presented. During the removal of a long strip of skin, the depth control of the dermatome was continuously adjusted so that a single strip contained sections of various thicknesses 200–650 μm, which included about 100 μm of epidermis. The strip was cut into several small sections about 2×2 cm^2, each with a different thickness. Each piece was soaked in normal saline (0.9 g NaCl/100 cc water) for at least 30 min to standardize the degree of hydration. It should be emphasized that such saline-soaked tissue, which is about 85 percent water, may not be optically equivalent to *in vivo* dermis, which is closer to 70 percent water. Soaking dermis will increase the backscattered reflectance from a sample [13]. The saline-soaked tissue, nevertheless, offered a standard, reproducible tissue preparation which

avoided the variations due to differences in water content between samples.

In the second set of experiments, skin was obtained from the abdomen at autopsy. The epidermis was manually separated following mild thermal treatment (2 min exposure in a 55°C water bath), which avoids thermal denaturation of dermal collagen. The dermal sample was frozen and cut with a cold dermatome to yield dermal sections 200–400 μm in thickness. The samples were soaked in saline prior to measurements. Specimens from five subjects were studied, with 9 measurements at different sites on each specimen.

In a third set of experiments, 6-mm diameter punch biopsies were obtained from abdominal human dermis collected at autopsy, and frozen and sliced parallel to the surface with a freezing microtome. Thicknesses of 20 μm were prepared at the level of the dermis, and several 20-μm sections were stacked to yield 40, 60, 80, and 100-μm thicknesses. Samples were held between two glass slides during measurements. Specimens from four subjects were studied: twenty-six samples with 20-μm thickness, nine 40-μm samples, four 60-μm samples, four 80-μm samples, and ten 100-μm samples.

Goniometric Apparatus

The goniometric apparatus for measuring the angular dependence of light scattering by tissue samples is shown in Figure 1. A HeNe laser, approximately 1 mW power at 632.8 nm, delivered a 1-mm diameter beam through a quartz window into the apparatus. The beam irradiated a tissue sample held between two glass slides in the center of the apparatus, which defined the origin of a radial coordinate system. A computer-controlled stepping motor positioned an optical fiber bundle at an angle θ relative to the forward on-axis direction of the laser beam in increments of 1.8°. The fiber was located at a radial distance, R_g, of 8.5 cm. The experiments were conducted with the tissue sample and detector immersed in saline to minimize refraction effects.

In the first experiment, the fiber bundle had a diameter of 1.55 mm, which presented a cross-sectional surface of 0.0189 cm^2 (a solid angle of 2.52×10^{-4} sr) for collection of light scattered by the tissue sample. The fiber bundle terminated 5 mm from a 1-cm^2 photodiode which measured all the collected light. In the second and third experiments, a 3-mm diameter fiber bundle was used, with a 1.17-mm diameter aperture, which restricted the collection area to a 0.0108-cm^2 area (a solid angle of 1.44×10^{-4} sr). The

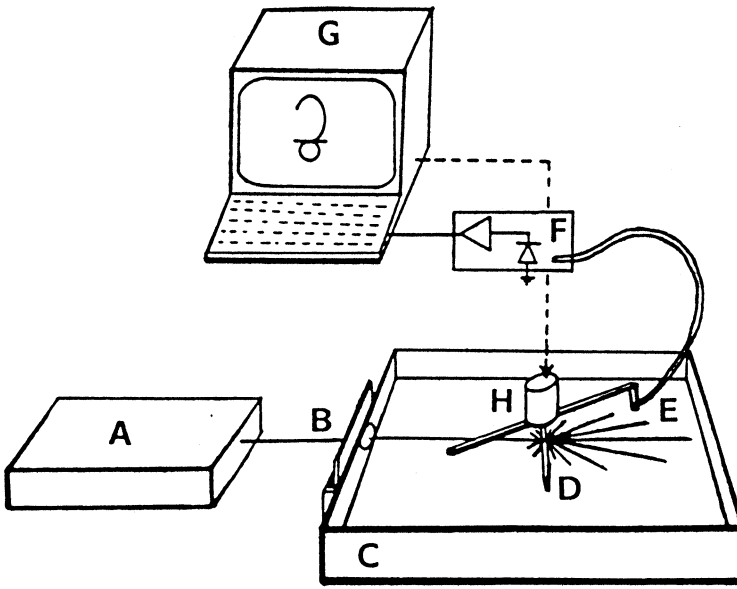

FIGURE 1 The goniometric apparatus for measurements of the angular dependence of light scattering by human dermis samples. A HeNe laser (A) delivers a collimated beam which enters through a port window (B) and strikes the tissue (D) held between glass slides at the center of the saline-filled tank (C). Scattered light is collected by an optical fiber bundle (E) which carries the light to a detector (F) (photodiode or photomultiplier) which is digitally monitored (G). A motor driven arm (H) under computer control rotates the collector bundle 360° around the sample.

fiber bundle terminated at a photomultiplier tube. During tissue measurements, the sample was placed in the center of the goniometer, and measurements were made 360° around the sample at 1.8° intervals. The measured half-maximum acceptance angle of the aperture/fiber bundle was ±20°, therefore the detector measured the integral of surface radiance from the entire sample surface.

The protocol began with a direct beam measurement of the total laser beam power with no sample at the origin, as the optical fiber bundle was held in front of the aperture to ensure complete capture of the entire beam. A filter with optical density 1.97 was placed in front of the laser during such direct beam measurements to avoid saturating the detector. Measurements of very thin tissue sections also required this filter.

The raw data was recorded as Voltages from the photodiode or photo-

multiplier tube operating in its linear range, and was subjected to a series of calculation steps described in Appendix 1. These calculations accounted for specular reflection and refraction effects due to the tissue/glass/saline interfaces. They yielded a description of the light that *exited* the tissue at a given angle θ_{exit}, as opposed to the light that was *observed* at a given angle θ_{obs} (see Fig. 2). The final result was the radiant intensity of light, $I(\theta_{exit})$ in units of W/sr for a 1-W incident beam, as it exited the tissue. In the following, we shall refer to θ_{exit} simply as θ.

RESULTS

Raw Data

The measured values of $P(\theta_{obs})$ for leg dermis are plotted in radial coordinates in Figure 3. The origin of each plot is located along an x-axis which

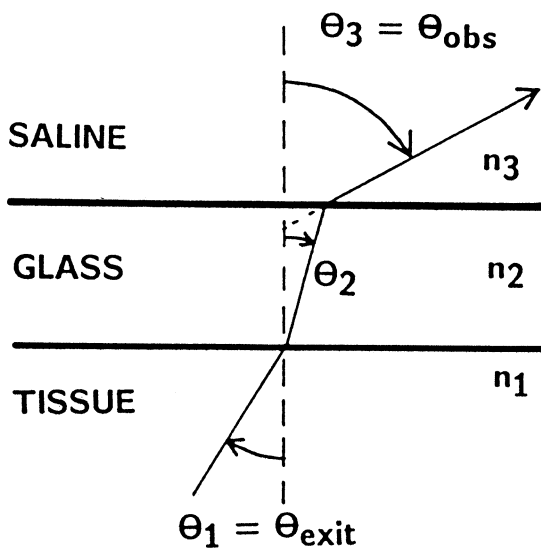

FIGURE 2 The refraction of light at the tissue/glass/saline interfaces as light escapes the tissue. The indices of refraction are 1.37 for dermis (70–85 percent water content), 1.54 for glass, and 1.33 for saline.

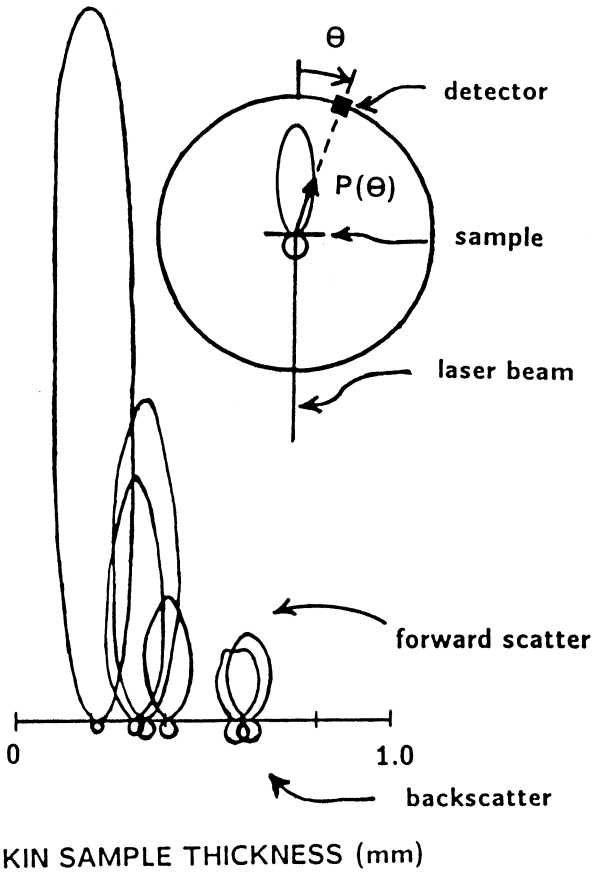

FIGURE 3 The observed radial plots of scattered light for tissue samples of various thicknesses (leg dermis). The goniometric measurement $P(\theta)$ is depicted schematically in the insert. The origin of each radial plot is positioned on the x-axis to indicate the sample thickness.

indicates the thickness of the sample. Each plot is the average value for measurements at several sites (6–10) on a given sample. The insert schematically illustrates the goniometric measurement. The thinner tissue samples yielded a very forward-directed scattering pattern, whereas the thicker samples greatly attenuated the on-axis intensity. At very oblique angles near $\pm 90°$, the observed scattered power decreased toward zero, which is charac-

teristic for observation of light emitted from a planar surface (Lambert's law of cosines) [15].

Equivalent Integrating Sphere Measurements

If scattering is assumed to be independent of azimuthal angle, the measured scattering function $P(\theta_{obs})$ may be integrated over all angles to yield the equivalent integrating sphere measurements of total transmission, T, and total reflectance, R. No azimuthal dependence of scattering was observed when the orientation of the tissue sample was rotated. The integrations yield T and R:

$$T = \frac{1}{2\pi R_g^2} \int_0^{\pi/2} [P(\theta_{obs})/\omega] 2\pi R_g \sin \theta_{obs} R_g d\theta_{obs}$$
$$R = \frac{1}{2\pi R_g^2} \int_{\pi}^{\pi/2} [P(\theta_{obs})/\omega] 2\pi R_g \sin \theta_{obs} R_g d\theta_{obs} \quad (1)$$

where $P(\theta_{obs})/\omega$ is the measured radiant intensity, and $2\pi R_g \sin(\theta_{obs}) R_g d\theta_{obs}$ represents an incremental ring of integration on the hemispherical surface specified by the goniometer arm. The values T, R, and $(T + R)$ from the first experiment (leg dermis) are plotted on a vertical log scale versus sample thickness in Figure 4. As tissue thicknesses increases, T decreases and R increases. The total absorption of laser energy in the tissue equals $[1 - (T + R)]$. The dashed lines are the theoretical curves calculated by the diffusion approximation solution (see Discussion). The slope of ln (T) versus thickness is linear, and the reciprocal slope is 14 cm^{-1} ($1/e$ depth of 710 θm within dermis).

Radiant Intensity Data

Figure 5A shows an example of detected values of $P(\theta_{obs})$ versus θ for a single tissue sample. Figure 5B shows the same data after use of Appendix 1 to yield the radiant intensity, $I(\theta)$ in W/sr for a 1 Watt laser beam, for light exiting the tissue. Note the strong forward on-axis intensity near θ equal 0°. There are no $I(\theta)$ data between $+105° < \theta < +74°$ and $-105° < \theta < -74°$ since total internal reflection at the glass/saline interface prevents light from reaching the detector at such oblique angles. The data at very oblique angles near ±90° were unreliable since (i) the signals were very small, and (ii) the

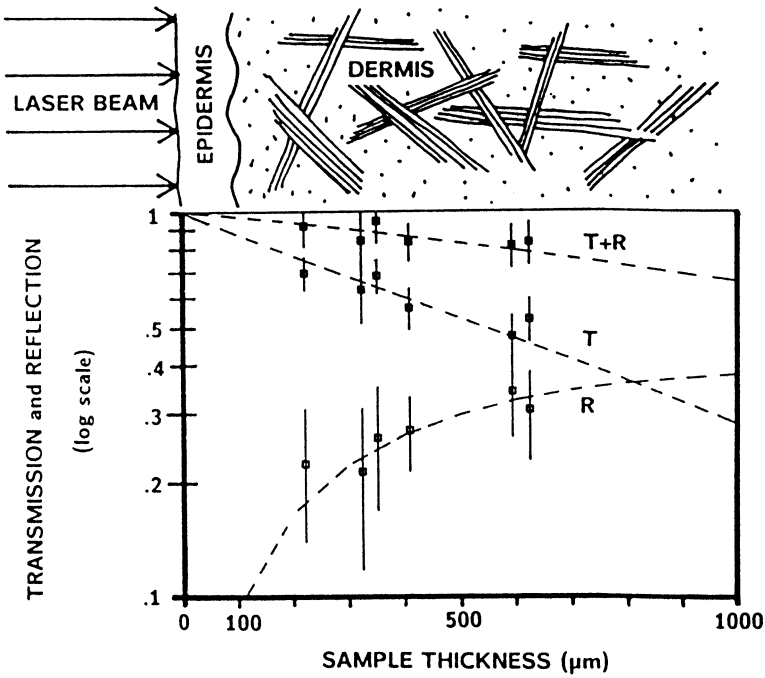

FIGURE 4 The equivalent integrating sphere measurements for HeNe laser transmission through full thickness human skin (leg dermis), calculated from the goniometric data using Eq. 2. The means and standard deviations of the transmission, T, reflection, R, and the total escaping flux, $R + T$, are shown on a log scale. The fitted lines are calculated by the diffusion approximation, using 2.7 cm^{-1} for the absorption coefficient, α, and the transformed parameters: the reduced scattering coefficient, σ', equal 22 cm^{-1}, and anisotropy, g', set to zero.

signals were normalized by $|\cos(\theta_{obs})|$ which approaches zero at θ_{obs} near $\pm 90°$. There is a slight constant intensity in the backscattered direction, $-180° < \theta < -105°$ and $-180° < \theta < +105°$, which indicates an isotropic scattering component. There is a small backward peak near 180°. This study did not attempt to resolve whether this backward peak was simply specular reflectance of the incident laser beam off the saline/glass interface or an example of retroflectance from dense scattering media [16].

The near on-axis pattern of scattered light is emphasized in Figure 6 for 20-μm-thick (mean of 19 measurements on 10 samples) and 280-μm-thick (mean of 9 measurements on 1 sample) dermal sections. The full-width half-

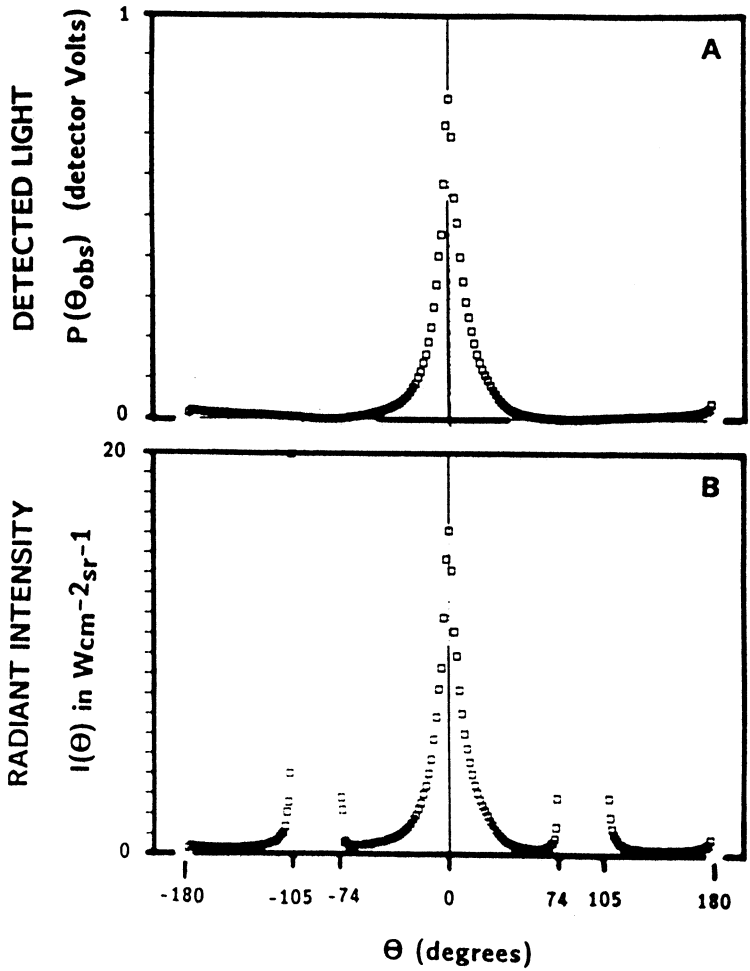

FIGURE 5 A, The detected scattered light, $P(\theta)$, versus the angle of observation, θ_{obs}, for a 280-μm-thick dermis sample (abdominal dermis). B, The scattered light intensity $I(\theta)$ versus the angle of exitance from the tissue (see Appendix 1). There is a pattern of strong forward-directed scattering around the on-axis ($\theta = 0°$) direction, superimposed on a slight isotropic scattering component characterized by the magnitude of backscattered light. There is no data between $\pm(75° < \theta < 105°)$ since total internal reflectance prevents light from exiting the tissue. The data appears noisy near ± 75° and ± 105° because so little light escapes the tissue for measurement, and a $1/|\cos(\theta_{obs})|$ factor amplifies the noisy data.

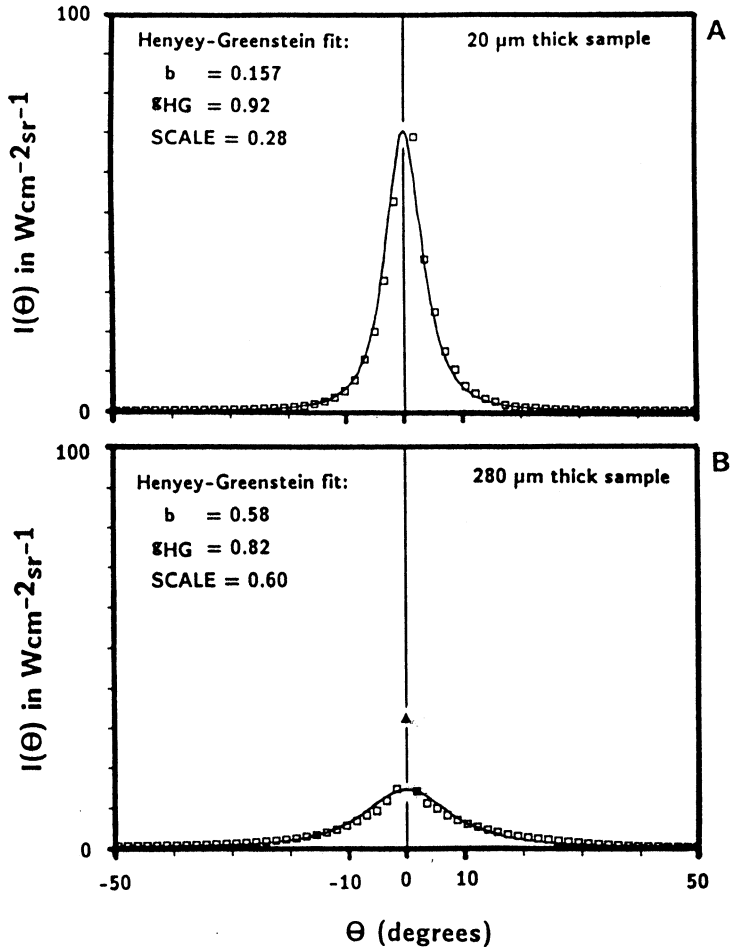

FIGURE 6 The radiant intensity of scattered light as a function of angle of exitance from the tissue (abdominal dermis). The solid lines are the best Henyey-Greenstein fits to the data. A, 20-μm thickness of dermis. B, 280-μm thickness of dermis. The on-axis value I_{total} (0°), which is shown as a solid triangle, includes the residual collimated laser beam which was not scattered.

max angle (FWHM) for the 20-μm samples is only 6.3°, but has broadened to 16° for the 280-μm sample. At θ equal 0°, there is an on-axis data point, $I_{total}(0°)$, which indicates the sum of the light scattered in the on-axis direction and the residual collimated laser beam not scattered by the tissue. This on-axis data point is offscale in Figure 6A (offscale at 3500 W/sr), but is shown in Figure 6B as a solid triangle at 33 W/sr. The modified Henyey-Greenstein function (see below), has been fitted to the data in Figure 6, excluding the on-axis point, and plotted as solid lines.

Henyey-Greenstein (H-G) Function

The I(θ) data can be conveniently represented by an analytic expression, the *Henyey-Greenstein* (H-G) function, which has been widely used in the atmospheric and marine literature to describe light scattering [17, 18]. The H-G function is not based on a mechanistic theory of scattering, but was chosen by Henyey and Greenstein to approximate Mie scattering. This convenient analytic expression depends on a single variable, g_{HG}, that varies between 0 and 1, as the scattering varies from an isotropic to a completely forward-directed scattering pattern. The correct use of the H-G function is to specify the phase function for a single scattering event. However, the $I(\theta)$ data for thicker samples which involve multiple scattering were also found to be well described by the H-G function, with only a slight modification to include an additional isotropic component:

$$I(\theta) = (\text{SCALE})\left[b + (1-b)\frac{1 - g_{HG}^2}{(1 + g_{HG}^2 - 2h_{HG}\cos u)^{3/2}} \right] (\text{W/sr}) \quad (2)$$

where b is the fractional component of isotropic scattering. This factor b was necessary to account for the amount of backscattered light in excess of that described by the H-G function, and was especially needed for the thicker samples, where multiple scattering increased the isotropic component. Again, the use of the H-G function to specify the radiant intensity $I(\theta)$ for thicker samples is only descriptive, and should be distinguished from the customary use of the H-G function to describe the single particle phase function.

The value of the term (SCALE)(b) was determined by the average radiant intensity in the backscattered angular intervals $+124° < \theta < +155°$ and $-155° < \theta < -124°$. SCALE is a scale factor which depends on the optical depth, $(\alpha + \sigma)d$, and albedo, $\sigma/(\alpha + \sigma)$, of the sample, where d is the tissue thickness, and α and σ are the absorption and scattering transport parameters, respectively, in units of cm^{-1}.

Analysis of goniometric data is facilitated by linearization of Eq. 2:

$$[I(\theta) - (\text{SCALE})(b)]^{-2/3} = \{-2g_{HG}/[A^{2/3}(1 - g_{HG}^2)^{2/3}]\} \cos\theta + (1 + g_{HG}^2)/[A^{2/3}(1 - g_{HG}^2)^{2/3}] \quad (3)$$

where A equals (SCALE)$(1 - b)$. Eq. 3 is in the form: $y = ux + v$ where x equals $\cos\theta$, u is the slope, and v is the y-intercept. Figure 7 illustrates analysis of a typical scan, plotting the left side of Eq. 3 versus $\cos\theta$. Least squares fitting to the data in the range $\cos\theta \geq 0.9$ yielded reliable values for u and v. The phase function parameters are specified:

$$g_{HG} = -(v/u) - (v^2/u^2 - 1)^{1/2}$$
$$\text{SCALE} = A + (\text{SCALE})(b) \quad (4)$$
$$b = (\text{SCALE})(b)/\text{SCALE}$$

where A equals $(-2g_{HG}/u)^{3/2}/(1 - g_{HG}^2)$, and (SCALE)$(b)$ was determined experimentally (above).

In Figure 8 the values (mean ± SD) for g_{HG}, b, and SCALE are plotted versus sample thickness, d. As the tissue thickness decreases, the scattering pattern becomes increasingly forward-directed, with g_{HG} increasing and b decreasing. In the limit of very thin tissue thicknesses below 100 μm, the scattering pattern is produced primarily by single scattering, and the values of g_{HG} and b approach constant values of about 0.91 and 0.10, respectively. The value of SCALE drops to zero in the limit of zero thickness. Its non-linear approach toward the origin is expected since the probability of a scattering event depends on tissue thickness, d, as $1 - \exp(-\sigma d)$.

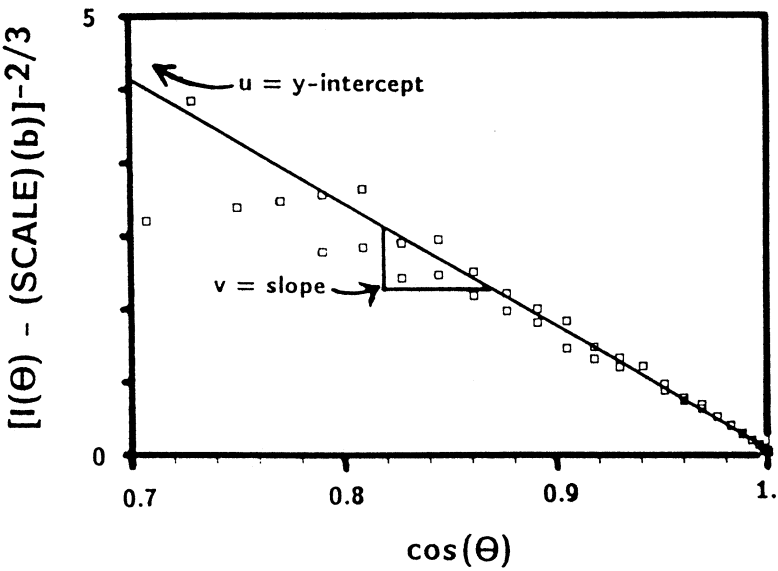

FIGURE 7 The method for specification of the Henyey-Greenstein function that describes light scattering for a particular tissue sample. The forward-directed component of the radiant intensity, $[I(\theta) - (\text{SCALE})(b)]^{2/3}$, is plotted versus cos (θ), where θ is angle of exitance (Eq. 3). Least squares fitting of the data where cos (θ) ≥ 0.9 yields the slope, v, and the y-intercept, u, which are used in Eqs. 10 to calculate g_{HG}, b, and SCALE. These example data are for a 20 μm-thick sample (abdominal dermis), and indicate g_{HG} equals 0.904.

On-axis Transmission

The on-axis transmission, $\exp[-(\alpha + \sigma)d]$, is attenuated by both scattering and absorption. The slope of the plot of ln[on-axis transmission] versus tissue thickness, d, indicates the magnitude of the total attenuation constant ($\alpha + \sigma$). Since α is very small at 632.8 nm, approximately 2.7 cm^{-1} [see Discussion], the calculated attenuation constant is primarily a specification of the value σ. In Figure 9, the values ln $[I_{total}(0°)]$ are plotted versus tissue thickness (open boxes and dashed line), and the reciprocal slope indicates that the attenuation constant equals 168 cm^{-1}. However, scattered light can also contribute to the observed on-axis transmission, as shown in Figure 6, therefore the true on-axis transmis-

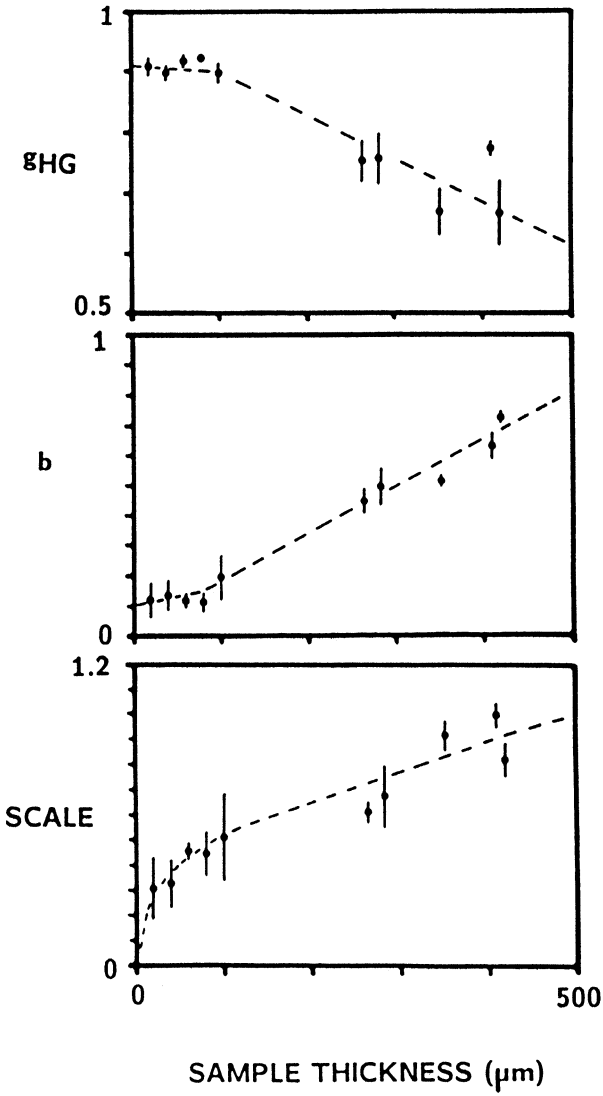

FIGURE 8 The Henyey-Greenstein parameters that describe the scattering function $I(\theta)$ versus sample thickness (see Eq. 2). The extrapolation to near zero thickness yields g_{HG} equal to 0.91, and b equal to 0.10. The amount of scattered light is represented by SCALE. (mean ± SD, abdominal dermis)

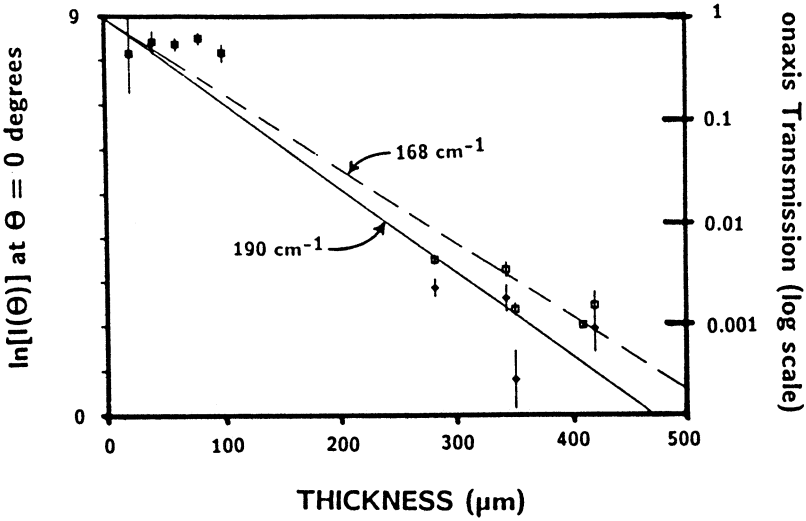

FIGURE 9 The logarithm of on-axis transmission versus dermis sample thickness (biopsies of abdominal dermis). The slope of the dotted line (open boxes) indicates an attenuation coefficient, $(\alpha + \sigma)$, of 168 cm^{-1}. The solid line (solid diamonds) shows the values after correction for the scattered light contribution to the on-axis transmission, and the slope indicates an attenuation coefficient of 190 cm^{-1}. The open boxes and solid diamonds become indistinguishable for sample thicknesses less than 100 μm.

sion of the original collimated beam must consider $[I_{total}(0°) - I(0°)]$, where $I(0°)$ is the on-axis magnitude of the scattered radiant intensity which is specified by the analytical H-G expression evaluated at θ equal 0°. The values $\ln [I_{total}(0°) - I(0°)]$ are also plotted versus tissue thickness (diamonds and solid line). The reciprocal slope of the solid line indicates that the true attenuation constant equals 190 cm^{-1}, and therefore σ is about 187 cm^{-1}. This implies that after 53 μm (equal to $1/\sigma$) about $1/e$ of the incident collimated photons have been scattered out of the on-axis cone of measurement.

DISCUSSION

As a photon travels through a thick sample of highly scattering tissue such as dermis, it will probably be scattered several times. If the thickness of the

sample is reduced, the average number of times the photon is scattered will drop. In the limit of an incremental sample thickness, the photon will be scattered once or not at all. Since the phase function used in the radiative transport equation describes the distribution of light scattered just once, the phase function is equal to the scattering function ($I(\theta)$ for an incremental tissue thickness divided by a normalization factor. Normalization is necessary because only the scattered light has contributed to the observed $I(\theta)$, and much of the incident light has passed through the sample undisturbed. Also, some absorption has occured since the albedo $\sigma/(\sigma + \alpha)$ is less than one, which further reduces the observed $I(\theta)$. The term SCALE in Eq. 2 accounts for these effects, and can be restated:

$$\text{SCALE} = \frac{1}{4\pi} \int_0^{\pi} I(\theta)\, 2\pi \sin\theta d\theta \tag{5}$$

The phase function is given:

$$p(\cos\theta) = p'(\theta) = I(\theta)/\text{SCALE} \tag{6}$$

where $I(\theta)$ is given by Eq. 2. The functions $p(\cos\theta)$ and $p'(\theta)$ differ only in that they use different domains: $\cos\theta$ versus θ. In the radiative transport equation, the phase function is usually described as $p(\mathbf{s} - \mathbf{s}')$ or $p(\cos\theta)$, where $\mathbf{s}$ and $\mathbf{s}'$ are the unit vectors for the directions of incidence and scatter, respectively, and $\mathbf{s} - \mathbf{s}'$ is their dot product. Eq. 6 ensures that the normalization condition for the phase function is satisfied, *i.e.* that the integral of the phase function over all angles is unity:

$$\frac{1}{4\pi} \int_0^{\pi} p'(\theta)\, 2\pi \sin\theta d\theta = 1 \tag{7}$$

A point of comparison between the above phase function and other phase functions, such as that used in the diffusion approximation,[9] is the anisotropy factor, g, which is defined as the average cosine of the phase function over all angles:

$$g = \frac{1}{4\pi} \int_{4\pi} p(\cos\theta) \cos\theta\, d(\cos\theta) \tag{8}$$

The value of g, like g_{HG}, varies from 0 for purely isotropic scattering to 1 for purely forward scattering, as if no scattering occurred at all. Substitution of Eq. 6 into Eq. 8 leads to the following relation for g in terms of the modified Henyey-Greenstein function parameters g_{HG} and b:

$$g = (1 - b)g_{HG} \tag{9}$$

For b equal 0.10 and g_{HG} equal 0.91, Eq. 9 yields a value 0.82 for g, which corresponds to an expectation value for cos θ, where θ equals 35°.

For comparison, we can cite a value for g in human dermis derived from unpublished measurements with a standard integrating sphere spectrophotometer and the diffusion approximation analysis following described methods.[1] Measurements at 632.8 nm on 40 human dermis samples of mean thickness 313 ± 82(SD) μm yielded a total transmission of 0.540 ± 0.058, and a total reflection of 0.243 ± 0.072 [19]. The value of $(\alpha + \sigma)$ equal to 190 cm^{-1} (Fig. 8), and the above integrating sphere measurements, T and R, together constitute three known values which allow three equations to be solved for the three unknowns: α, σ, and g [1]. Because the samples were held between glass slides in the spectrophotometer, values for the internal reflectance, r_i, at the front and back tissue/glass/air interfaces must also be assumed as scattered light attempted to exit the sample. In the following two paragraphs, we use the goniometric measurements to estimate these values for r_i using Fresnel's law.

The value for r_i can be calculated for reflection of an internal irradiance that can vary between purely diffuse to purely collimated, as described by the radiant intensity, $I(\theta)$, striking an arbitrarily small surface area at the interface:

$$R_i = 1 - \frac{\int_0^{\theta_{crit}} I(\theta)t(\theta) \cos\theta \, 2\pi \sin\theta d\theta}{\int_0^{\pi/2} I(\theta) \cos\theta \, 2\pi \sin\theta d\theta} \tag{10}$$

where $I(\theta)$ is given by Eq. 2, $t(\theta)$ is the transmission specified by Fresnel's law for randomly polarized light striking the tissue/glass/saline interface (Eq. A6, Appendix 1), $\cos\theta$ represents the receiving function for the incremental surface, $2\pi\sin\theta d\theta$ represents an incremental ring on the hemisphere of integration, and θ_c is the critical angle for total internal reflectance (Eq. 10 is similar to Eq. 74 in Ryde [20], and to Eq. 3.1 in Giovanelli [21], but allows treatment of the three layer problem: tissue/glass/air). To test Eq. 10, calculation of r_i for an ideally diffuse internal irradiance at an opal glass/air interface where the glass has an index of refraction equal to either 1.50 or 1.60, yields 0.596 and 0.651, respectively, which agree with the values reported by Giovanelli [21] and Judd [22] to within ±0.001. Experimental values in the literature for r_i for an opal glass/air interface range between 0.4–0.5 [23, 24], which are lower than the theoretical value and may indicate the difficulty in experimentally establishing a truly diffuse internal

irradiance near an interface. Calculation of r_i for a diffuse internal irradiance at either a water/air or a water/glass/air interface ($n = 1.54$ for the glass) yields 0.472 and 0.493, respectively.

The goniometric data indicated that the backscattered light that exited the front sample surface was approximately isotropic. The value for r_i is calculated by Eq. 10 to be 0.521 for an ideally diffuse internal irradiance at a tissue/glass/air interface. The irradiance transmitted to the back side of the tissue samples was not completely diffuse. The goniometric experiments (Fig. 8) indicated that the irradiance transmitted through such thick samples should exhibit an angular dependence described by the modified H-G function, where g_{HG} is 0.75 and b is 0.5 for an average 313-μm thick dermal sample. Application of Eq. 10 to such an anisotropic irradiance yields an r_i of 0.239 for the back side of the tissue sample. The specular reflectance, r_s, of the collimated beam in the spectrophotometer is 0.048, based on Eq. A1 in Appendix 1 for a tissue/glass/air interface.

These values for r_s and r_i at the front and back surfaces cause the diffusion approximation analysis to yield the following transport parameters: $\alpha = 2.7$ cm^{-1}, $\sigma = 187.3$ cm^{-1}, and $g = 0.807$. This value for g agrees well with the 0.82 value based solely on the goniometric measurements and Eq. 9. We tentatively conclude these values represent the optical transport parameters for human dermis at 632.8 nm. Table I summarizes the results.

The above transport parameters for bloodless dermis can be used to predict the total radiant energy fluence rate, Φ in Wcm^{-2}, as a function of depth for a broad 1-Wcm^{-2} beam. The value Φ is defined as $C + 2(I + J)$, where C, I, and J are the collimated, forward-diffuse, and backward-diffuse energy fluence rates, respectively, and $\alpha\Phi$ yields the absorbed energy density in W/cc.[1] The transport parameters have been used in both Monte Carlo calculations and the 1D diffusion approximation solution [24]. Under matched boundary conditions, the two calculations agree on the predicted reflectance and Φ at the skin surface, but disagree on the internal spatial distribution of Φ. The diffusion theory overestimates the magnitude of the subsurface peak in Φ when the calculation uses a large g value such as 0.8. However, when the diffusion theory calculation uses transformed scattering and anisotropy parameters, the reduced scattering coefficient, σ' defined as $\sigma(1 - g)$, and an anisotropy g' set to zero, then it predicts values for Φ throughout the tissue which agree with Monte Carlo calculations that use the original σ and g values. The use of such transformed transport parameters is consistent with the "Similarity Principle" [17]. The calculated internal distribution of Φ agrees with experiments which indicate only a slight

TABLE I

Transport Parameters at 632.8 nm

Goniometric Expts. and Henyey-Greenstein		Integrating Sphere Expts. [19] and Diffusion Approximation	
Measurements:			
g_{HG}	0.91	T	0.540 ± 0.058
b	0.10	R	0.243 ± 0.072
		d	323 ± 82 μm (mean ± SD, n = 40)
$(\alpha + \sigma)$	190 cm^{-1}		
use: $g = (1 - b)g_{HG}$		use: $\alpha + \sigma = 190\ cm^{-1}$	$r_i = 0.521$ at front, $r_i = 0.239$ at back, $r_s = 0.048$
Calculated parameters:			
		α	2.7 cm^{-1}
		σ	187.3 cm^{-1}
$g \equiv \langle \cos\theta \rangle$	0.82	g	0.807
$\langle \theta \rangle$	35.0°	$\langle \theta \rangle$	36.2°

subsurface peak in Φ is possible [25]. In Figure 10 the Φ distributions agreed upon by both calculations are shown for *in vivo* irradiation of human skin (neglecting the epidermis and dermal blood volume) by a broad collimated beam at 632.8 nm, incident Φ equal 1 W/cm^2. A water/skin interface is assumed which provides relatively good index matching so that internal reflectance can be neglected ($r_i \simeq 0$). Because the dermis is quite thick (4 mm), the reflectance at the dermis/fat/fascia interface does not influence the distribution of Φ in the first 1 mm of tissue. The value of Φ at the skin surface is 1.97 W/cm^2. A slight subsurface peak in Φ occurs at a depth of 100 μm, where Φ equals 2.05 W/cm^2. Beyond this peak, Φ decays exponentially with an attenuation constant, k_d:

$$k_d = [3\alpha\{\sigma(1 - g) + \alpha\}]^{1/2} \tag{11}$$

which equals 18 cm^{-1} (1/e = 560 μm).[1] Only at a depth of 0.8 mm does Φ finally drop to a value equal to the incident collimated Φ, therefore the actual depth at which Φ has dropped to $1/e$ of the incident Φ is about 1.4 mm.

The model can also reconstruct the equivalent integrating sphere transmission and reflectance data for finite tissue thicknesses (Fig. 4, leg dermis) by repeating the calculations for various thickness, d, with matched boundaries

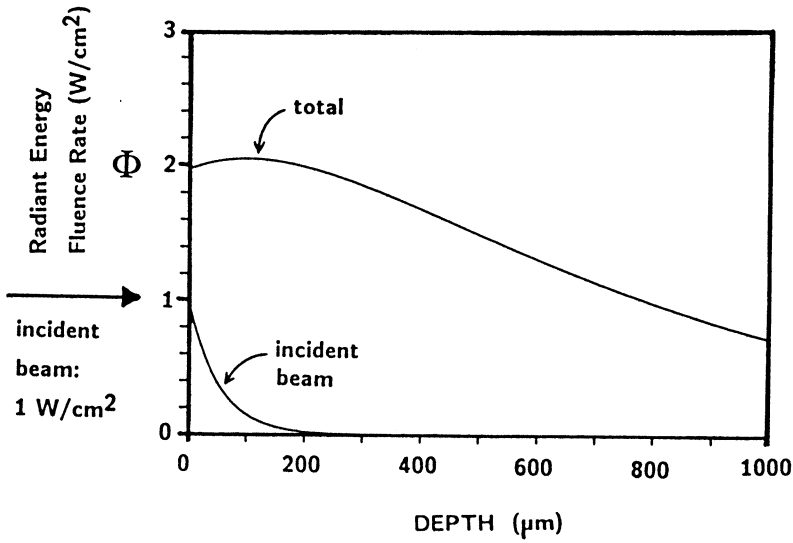

FIGURE 10 The light distribution within human abdominal dermis under matched boundary conditions (*e.g.*, a water/skin interface). The incident collimated beam is rapidly attenuated by both scattering and absorption. The total radiant energy fluence rate, Φ, penetrates deeply into the dermis. Calculation is based on the 1D diffusion approximation solution to the transport equation using the parameters: absorption coefficient $\alpha = 2.7\ cm^{-1}$, and the transformed parameters: reduced scattering coefficient $\sigma' = 36\ cm^{-1}$ ($\sigma' = \sigma(1 - g)$, where $\sigma = 187\ cm^{-1}$ and $g = 0.81$), and anisotropy g' set to zero.

and assuming α and σ' equal 2.7 and 22 cm^{-1}, respectively. The value of k_d is 14 cm^{-1} ($1/e = 710\ \mu m$), which suggests less scattering for the leg dermis sample than for the abdominal samples. More work on the variation in dermal optical properties for various aged subjects and different body locations is required.

CONCLUSION

The goniometric apparatus and calculation methods described in this report offer a means to specify the scattering coefficient and phase function for a tissue, and experiments in this report have characterized light scattering (632.8 nm) in human dermis. By documenting how sample thickness affects the angular dependence of light scattering, extrapolation to an incremental

tissue thickness has yielded the phase function for use in the transport equation. Both the isotropic and forward-directed components of the phase function have been characterized. By correcting the on-axis transmission measurements for the amount of scattered light that is still collected on-axis, based on the scattering function for each sample, the total attenuation coefficient for the incident collimated light has been specified for human dermis. Good agreement is found between the values for anisotropy, g, based on the goniometric measurements and those based on the integrating sphere measurements and diffusion approximation analysis.

Although dermis rapidly scatters an incident collimated laser beam, the forward-directed nature of light scattering permits photons to continue their penetration into dermis despite the loss of collimation. Therefore, the total radiant energy fluence rate, Φ, is attenuated only slowly. Rapid attenuation of the on-axis Φ of very narrow laser beams in dermis occurs due to radial spread of the beam caused by scattering, while broad laser beams will successfully penetrate to deeper targets.

Acknowledgments

We thank Martin van Gemert, Willem Star, Hans Marijnissen, Myron Wolbarsht, and Franz Hillenkamp for helpful discussions; A. J. Welch and John Parrish for their interest and facilitation in the collaboration of our laboratories; Dave Zrakit for the integrating sphere measurements; Phil Devlin at the Skin Bank of the Shriners' Burn Institute for the dermal samples from the leg; Peggy Sherwood and Faith Caverly for the tissue preparations with the freezing microtome.

References

1. Jacques S. L. and Prahl S. A.: Modeling Optical and Thermal Distributions in Tissue During Laser Irradiation. *Lasers in Surgery and Medicine* **6**, 494–503, 1987.
2. Langerholc J.: Moving Phase Transitions in Laser-irradiated Biological Tissue. *Applied Optics* **18**, 2286–2293, 1979.
3. Garden J. M., Tan O. T., Kershmann R., Boll J., Furimoto H., Anderson R. R., and Parrish J.A.: Effect of dye laser pulse duration on selective cutaneous vascular injury. *J. Invest. Dermatol.* **87**, 653–657, 1986.
4. Polla L. L., Jacques S. L., Margolis R. J., Prince M. R., Anderson R. R., Parrish J. A., and Tan O. T.: Photothermolyse Selective: Application au Traitment des Angiomes Plans par le Laser. *Annales de Dermatologie* (in press), 1986.
5. van Gemert M. J .C., Welch A. J., and Amin A. P.: Is There an Optimal Laser Treatment for Port Wine Stains? *Lasers in Surgery and Medicine* **6**, 76–83, 1986.
6. Anderson R. R., Hu J., and Parrish J. A.: Optical Radiation Transfer in the Human Skin and Applications in *in vivo* Remittance Spectroscopy. In Marks, R., Payne, P. A., and

Press, M. T. P. (Eds.): *Bioengineering and the Skin*. Hingham, MA: Kluwer Boston Inc., p. 253–265, 1981.
7. Anderson R. R. and Parrish J. A.: The Optics of Human Skin. *J. Invest. Dermatol.* **77**, 13–19, 1981.
8. Kottler F.: The Elements of Radiative Transfer. *Progress in Optics* **3**, 1–28, 1964.
9. Ishimaru A.: *Wave Propagation and Scattering in Random Media*. New York: Academic Press, 1978.
10. Bruls W. A. G. and van der Leun J. C.: Forward Scattering Properties of Human Epidermal Layers. *Photochem. Photobiol.* **40**, 231–242, 1984.
11. Wilksch P. A. and Jacka F.: Studies of Light Propagation through Tissue. In *Porphyrin localization and treatment of tumors*. Alan R. Liss, Inc., p. 149–161, 1984.
12. Parrish J. A.: New Concepts in Therapeutic Photomedicine: Photochemistry, Optical Targeting and the Therapeutic Window. *J. Invest. Dermatol.* **77**, 45–50, 1981.
13. Jacques S. L. and McAuliffe D. J.: Non-invasive Quantification of Cutaneous Edema *in vivo* with a 1 GHz Dielectric Probe. Joint International Meeting of the Society for Investigative Dermatology and the Japanese Society for Investigative Dermatology, May, 1985. *Clin. Res.* **33(2)**, 650A, *J. Invest. Dermatol.* **84**, 359, 1985.
14. Bausch and Lomb: "Refractive Index and Percent Dissolved Solids Scale." Analytic Systems Division (S-5195 0675)
15. Born M, and Wolf E.: *Principles of Optics*. Oxford: Pergamon Press, p. 19
16. Kuga Y. and Ishimaru A.: Retroflectance from a Dense Distribution of Spherical Particles. *J. Opt. Soc. Am. A.* **1**, 831–835, 1984
17. van der Hulst H. C.: *Multiple Light Scattering: Tables, Formulas, and Applications*. 2 volumes. New York: Academic Press, 1980.
18. Henyey L. G. and Greenstein, J. L.: Diffuse Radiation in the Galaxy. *Astophysical J.* **93**, 70–83, 1941.
19. Jacques S. L., Zrakit D., and Prahl S. A.: Wavelength Dependence (350–800 nm) of Optical Transport Parameters for Human Dermis. Manuscript in preparation.
20. Ryde J. W.: The Scattering of Light by Turbid Media. Part I. *Proc. Roy. Soc. London* **A131**, 451–464, 1931.
21. Giovanelli R. G.: A Note on the Coefficient of Reflection for Internally Incident Diffuse Light. *Opt. Acta* **3**, 127–130, 1956.
22. Judd D. B.: Fresnel Reflection of Diffusely Incident Light. *J. Res. Nat. Bur. Stand.* **29**, 329–332, 1942.
23. Kottler F.: Turbid Media with Plane-parallel Surfaces. *J. Opt. Soc. Am.* **50**, 483–490, 1960
24. Ryde J. W. and Cooper B. S.: The Scattering of Light by Turbid Media. Part II. *Proc. Roy. Soc. London* **A131**, 464–475, 1931.
25. Jacques S. L., Farinelli, W. A., Long, F. H., Deutsch, T. F., and Anderson, R. R.: The Spatial Distribution of Optical Energy in Tissue Deduced from Irradiometry of Surface Temperature after Pulsed Laser Irradiation. 2nd European Congress of Photobiology, Padua, Italy, Sept 6–11, 1987.

APPENDIX 1

The experiments involved a tissue sample held between two glass slides and submerged in saline. Therefore, the specular reflectance and refraction at the tissue/glass/saline boundary must be considered, and values for the indices of refraction, n_{tissue}, n_{glass}, and n_{saline}, must be assumed. The following

expression gives the net transmission across the two interfaces between three media with indices of refraction, n_1, n_2, and n_3:

$$T_{net} = (1 - R_1)(1 - R_2)[1 + \sum_{i=1}^{\infty} R_1^i R_2^i] \quad \text{(A1)}$$

where $R_1 = (n_1 = n_2)^2/(n_1 + n_2)^2$
$R_2 = (n_2 - n_3)^2/(n_2 + n_3)^2$.

The n_{glass} was measured to be 1.54. The tissue value, n_{tissue}, was based on the generalization that the index of refraction of a tissue varies linearly between 1.33 to 1.5 for water contents between 100 percent andto 0 percent [14]. The value n_{tissue} would vary from 1.38 to 1.36 as water content varies from 70 to 85 percent, and we used the value 1.37. The assumed value for n_{saline} was 1.33. Application of Eq. A1 for the tissue/glass/saline combination yields a T_{net} of 99.1 percent, which we later refer to as a specular reflectance, r_s, equal to 0.9 percent.

The raw data was subjected to a series of calculation steps to achieve a description of the light that *exited* the tissue at a given angle θ_{exit}, as opposed to the light that was *observed* at a given angle θ_{obs} (see Fig. 2).

(1) The raw data, recorded as Volts (V) but representing collected power in Watts, was normalized by the direct beam measurement, V_{DB}, to yield the collected power relative to a 1 Watt incident beam. Division by $(1 - r_s)$ corrected for the specular reflectance ($r_s = 0.009$) from the front glass slide as the incident beam entered the tissue:

$$P(\theta_{obs}) = V(\theta_{obs})/[V_{DB}(1 - r_s)] \quad \text{in W} \quad \text{(A2)}$$

(2) The collected power was divided by the solid angle of collection by the optical fiber bundle, ω equal to $4\pi(A_d/4\pi R_g^2)$ steradians. Here A_d was the collection area of the fiber bundle, and R_g was the radius of the goniometer rotating arm. This calculation yielded the observed radiant intensity $A(\theta_{obs})$:

$$A(\theta_{obs}) = P(\theta_{obs})/\omega \quad \text{in W/sr} \quad \text{(A3)}$$

(3) The observed radiant intensity was corrected by $|\cos \theta_{obs}|$ to account for the viewing angle, since observation of light emitted from a planar surface is diminished at oblique angles, according to a cos (θ) factor:

$$B(\theta_{obs}) = A(\theta_{obs})/|\cos \theta_{obs}| \quad \text{in W/sr} \quad \text{(A4)}$$

(4) The value $B(\theta_{obs})$ was then corrected for the refraction at the tissue/glass/saline interfaces which caused the solid angle to expand as light exited the tissue, especially at oblique angles of observation, and consequently diminished the observed radiant intensity:

$$C(\theta_{obs}) = B(\theta_{obs})[(\theta_{max} - \theta_{min})/b]^2 \text{ in W/sr} \quad \text{(A5)}$$

$$\text{where } \theta_{max} = \sin^{-1}[\sin(\theta_{obs} + b/2)n_3/n_1]$$
$$\theta_{min} = \sin^{-1}[\sin(\theta_{obs} - b/2)n_3/n_1]$$
$$b = D/R_g \text{ radians,}$$

where D is the diameter of the collection area of the fiber bundle.

(5) The value $C(\theta_{obs})$ was corrected for Fresnel reflection at the tissue/glass and glass/saline interfaces, which allowed only a fraction, $t(\theta)$, of the light to escape and reach the detector:

$$I(\theta_{obs}) = C(\theta_{obs})/t(\theta) \text{ in W/sr} \quad \text{(A6)}$$

$$\text{where } t(\theta) = (1 - r_1)(1 - R_2)\left[1 + \sum_{i=1}^{\infty} R_1{}^i R_2{}^i\right]$$
$$r_i = (\tfrac{1}{2})[\tan^2(\theta_i - \theta_i{}^+{}_1)/\tan^2(\theta_i + \theta_{i+1}) + \sin^2(\theta_i - \theta_{i+1})/\sin^2(\theta_i + \theta_{i+1})]$$
$$\text{for } i \text{ equal 1 or 2,}$$

where the angles θ_1, θ_2, and θ_3 as shown in Figure 2 were calculated by application of Snell's law:

$$\theta_3 = \theta_{obs}$$
$$\theta_2 = \arcsin(\sin(\theta_3)n_3/n_1)$$
$$\theta_1 = \arcsin(\sin(\theta_2)n_2/n_1)$$

The above calculation of $t(\theta)$ considers the multiple reflections within the glass slide between the tissue/glass and glass/saline interfaces.

(6) The value $I(\theta_{obs})$ was then attributed to the true angle of exitance from the tissue, θ_{exit}, as opposed to the observed angle, θ_{obs}, in consideration of the refraction at the tissue/glass and glass/saline interfaces:

$$\theta_{exit} = \theta_1 \quad \text{(A7)}$$

The final result of this series of calculations was the radiant intensity of light, $I(\theta_{exit})$ in units of W/sr for a 1 W incident beam, as it exited the tissue. In the text, we shall refer to θ_{exit} simply as θ.

These corrections (Eqs. A2–A7) become important only at widely scattered angles. For comparison, consider the magnitude of the net correction factor based on these equations for a given angle θ_{obs}, relative to the factor for the forward on-axis direction. At 20°, the relative correction factor is only 1.07, primarily due to the $1/\mid \cos\theta \mid$ term of Eq. A4. At 45°, the relative correction factor is 1.41, and 91 percent is due to Eq. A4. But at 70°, the factor is 2.94, and only 32 percent is due to Eq. A4. The other refraction effects are now more important than the correction for Lambert's law. These equations enable proper evaluation of the widely scattered light.